

Chapter 6

Characterization of PMMA/TiO₂ composites

Abstract

This chapter gives an account of the characteristics of PMMA/TiO₂ composites in different weight proportion (0.03%, 0.1% and 0.5% of TiO₂) which is prepared by solution cast technique. These blends are investigated by spectroscopic techniques like FTIR and UV-Vis. Mechanical, Thermal and Morphological properties are also investigated. The results obtained from different characterization techniques show the doping effect on different properties. These properties of composites are correlated with spectroscopic investigation.

6.1. Introduction

Polymeric materials are cheaper and easier to process as well as they are convenient to assemble. The benefits of lightweight polymeric materials over metallic materials are well known. Polymers are of deep interest to society and are replacing metals in diverse fields of life, which can be further modified according to modern applications. As we know, incorporating inorganic particles into polymer matrix is a practicable way to obtain advanced materials of composite [1]. In recent years, organic/inorganic composite materials have attracted considerable attention in both scientific and industrial circles, because they offer attractive potential for diversification and application of traditional polymeric materials [2, 3]. Organic–inorganic hybrid materials are hi-tech because they can present simultaneously both the properties of an inorganic molecule besides the usual properties of polymer. These hybrid materials sometimes lead to unexpected new properties, which are often not exhibited by individual compounds and thus open a new avenue for chemists, physicists and materials scientists [4]. These hybrid materials are new, versatile class of materials, exhibiting a vast application potential, due to their tailorable mechanical, optical and electrical properties [5-7].

When two different kinds of materials are used in combination to improve one or more properties of the component material is called composites. Composites materials are generally consist of a continuous phase which is surrounded by dispersed phase. Changes in size of dispersed phase (macroscopic to nano) reflect changes in physical properties. Homogeneity improves for smaller dispersed phase. Composite materials can be classified by the chemical interactions between the two phases. Kickelbick [8] used the strength of the intermolecular forces to classify the types of hybrid materials formed, contrasting those with chemical bonding between phases, weaker intermolecular forces between phases, or those with little or no

interaction between the phases. Interaction between the inorganic and the organic phase by hydrogen bonding in hybrid materials exists. The structure of the different classes varies widely and includes a dispersion of the inorganic in the continuous phase, an interpenetrating network of inorganic component and polymer, pendant inorganic groups attached to the polymer backbone, and true hybrids, described as structures where covalent bonds exist between inorganic and organic phase [9]. These differences in structure can affect the pyrolysis behavior of the hybrid material. The mechanical properties of particulates-filled polymers are significantly influenced by interfacial interactions, which depend on the interfacial compatibility and interfacial adhesion between the particulates and the matrix [10]. In recent years, studies on optical and electrical characteristics of polymers have fascinated much consideration in their application in optical and electronic devices [11]. The optical properties of the polymers can be correctly customized by the addition of dopant depending on their reactivity with host matrix. Optical parameters (e.g. refractive index, optical band gap, etc.) of poly methyl methacrylate (PMMA) depend on its molecular structure and they can be modified. Titanium dioxide or Titania (TiO_2) is a harmless white material widely used in photo electrochemical solar energy conversion and environmental photo catalysis (treatment of polluted water and air) including self cleaning and anti fogging surfaces [12, 13]. It is also commonly used as a high refractive index material in optical filter applications and sensors [14, 15]. Nano structured TiO_2 is used in solar cell research and displays [16]. TiO_2 thin films are valued for their good durability, high dielectric constant, high refractive index, excellent transparency in the visible range and biocompatibility. In polymer light emitting diode devices, mixing TiO_2 nanoparticles into poly [2-methoxy-5-(20-ethyl-hexyloxy) - para-phenylenevinylene] MEH-PPV results in increased current densities, radiances and power efficiencies [17, 18]. Electrical and optical properties of polyvinyl alcohol thin films doped with metal salts have been investigated by Abd et al.[19]. Refractive index is an important optical



parameter for the design of prisms, windows and optical fibers [20]. The absorbance process plays an important role in the optical properties of polymers. From the absorption spectra, it is possible to understand variation of molecular formation of polymer structures.

The study of the optical absorption spectra in solids provides necessary information about the band structure and the energy gap in the crystalline and non-crystalline materials. Analysis of the absorption spectra in the lower energy part gives information about atomic vibration while the higher energy part of the spectrum gives knowledge about the electronic states in the atom [19].

A. Qureshi et al. studied optical and electrical properties of polypropylene/TiO₂ composites [21].

The band gap width (E_g) depends on many parameters, e.g. on crystallinity of materials, on their anisotropy, temperature, pressure, on effect of external electric and magnetic forces [22]. A similar change of optical energy band gap in polymers was published under doping PMMA with metal halogenides [23], after ions implantation in polyimide [24], and after implanting electrons or protons in PP, PTFE, PET, PI [25].

Here PMMA/TiO₂ system was chosen as a model to prepare inorganic/ polymer composites. Preparation and characterization of the PMMA/TiO₂ composites is described in this chapter. The structural, optical, mechanical, thermal and morphological properties are studied. The analyses confirmed the good dispersion of TiO₂ particles in PMMA polymer matrix and making successfully composites films with good properties.

6.2. Results and Discussion

6.2.1. FTIR Analysis

FTIR (Fourier transform infrared) spectroscopic techniques are used to quantitatively assess polymer interactions for many years. Infrared spectroscopy is a tool to find out the possible interaction between the polymer and inorganic dopant. In addition to FTIR's simplicity and

universal use, the frequencies of bands and the band shape are directly related to microscopic physical quantities and hence from the spectra we can correlate the other properties. The interaction can be studied by noting the shift of the peaks, developments of new peaks, changes in shapes like changes in peak intensity, development of shoulders in the existing peaks in the FTIR spectrum [26-28].

Table 6.1 Assignment of different vibrational modes of PMMA and its various composites.

Vibrational Modes ↓	Wave number (cm ⁻¹)				
	TiO ₂ % in PMMA polymer →	0%	0.03%	0.1%	0.5%
-CH ₂ rocking		733	732	733	732
-CH ₂ rocking with skeleton stretching		750	750	750	750
Ti-O-C vibration			809	810	810
C-C stretching		841	841	840	841
C-O stretching		1140	1140	1140	1140
-CH ₃ symmetric stretching		1387	1384	1387	1388
-COO ⁻ stretching		1435	1434	1434	1434
-CH ₃ bending		weak	1441	1446	1446
-CH ₂ bending coupled with -CH ₃ bending		1487	1482	1480	1480
C=O stretching		1719	1722	1721	1721
-CH ₂ symmetric stretching			weak	2925	2922
O-CH ₃ symmetric stretching		2948	2950	2950	2950
-CH ₂ asymmetric stretching		2993	2995	2993	2990

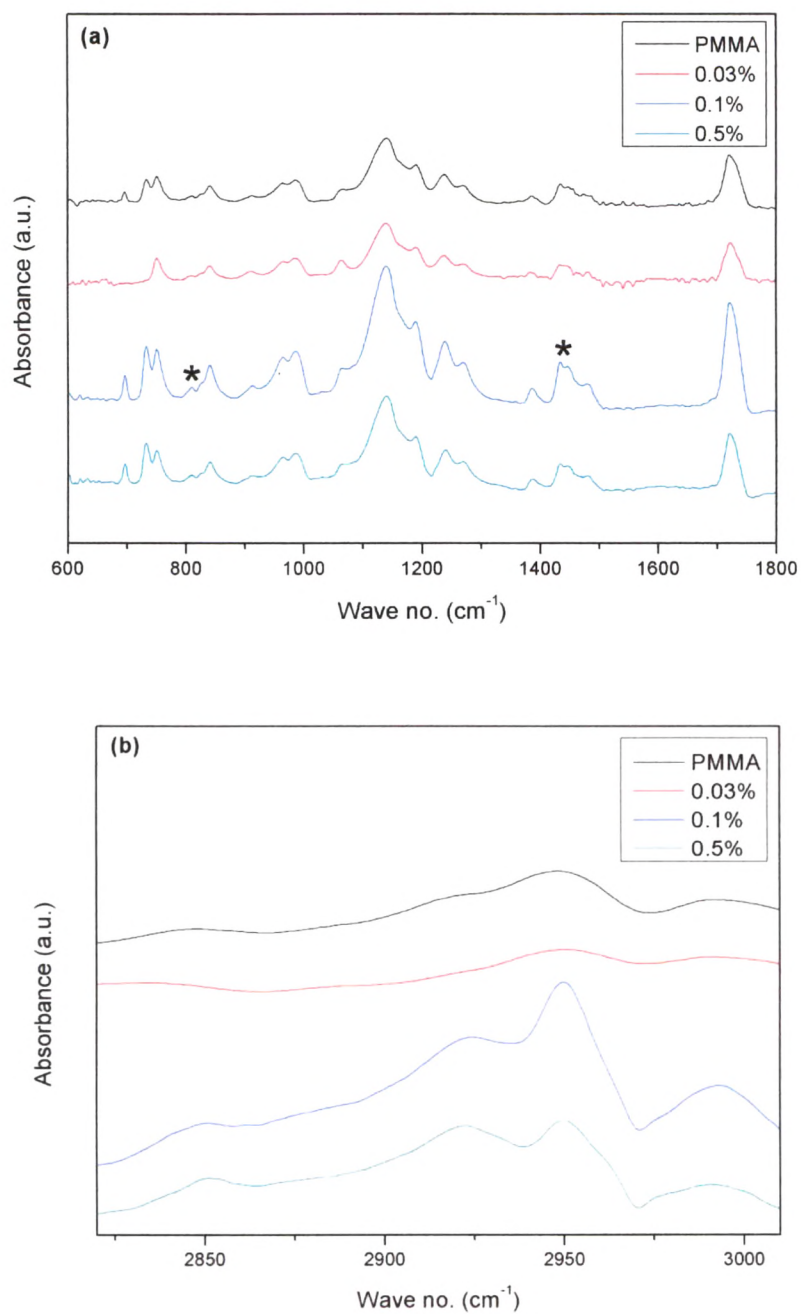


Figure 6.1 FTIR Spectra of pure PMMA and Their composites (a) in the range 600 – 1800 cm^{-1} (b) in the range 2800 – 3000 cm^{-1}

In this section, FTIR spectra were employed to identify the chemical interaction of PMMA/TiO₂ composite films of various composition ratios. FTIR spectra are presented in **Figure 6.1**. The vibrational mode assignment with their values for pure PMMA and their composites are shown in **Table 6.1**. The band at 809 cm⁻¹ (marked as * in **Figure 6.1**) appears for composites only, which is due to Ti-O-C vibration. The peak around at 1443 cm⁻¹ and 1487 cm⁻¹ for PMMA attributed to -CH₃ bending and -CH₂ bending coupled with CH₃-O bending respectively, whereas the -CH₃ stretching vibration is centered at 1387 cm⁻¹[29]. Peak at 1435 cm⁻¹ (marked as * in **Figure 6.1**) become prominent in composites sample which is due to carboxylate (-COO⁻) stretching. This clearly indicates the interaction between PMMA and TiO₂ which confirmed the results obtained by Annalisa Convertino et. al.[30]. Characteristic absorptions due to the stretching of ether (C-O) carbon and carbonyl (C=O) of the ester group are observed at 1140 cm⁻¹ and 1719 cm⁻¹ for all the composites with changes in absorption intensity. Carbonyl peak's shape and intensity are changed for composites. This is due to the coordination of Ti⁺⁴ with carbonyl oxygen on the ester side of PMMA that is acting as a transient crosslink [29]. Two bands 2925 cm⁻¹ and 2993 cm⁻¹ are appearing due to -CH₂ stretching modes of PMMA, **Figure 5**. The asymmetric stretching mode at 2993 cm⁻¹ and symmetric stretching mode at 2925 cm⁻¹ of -CH₂ group exhibits noticeable changes in intensity for the composites with TiO₂ filler. Intensity of the absorption of these peaks increases (as compare to pure PMMA) with TiO₂ addition and maximum for 0.1% of TiO₂. The peak at 2925 cm⁻¹ is lacking in pure PMMA and almost disappears for 0.03% as seen in **Figure 6.1 (b)**: The 2950 cm⁻¹ peak's intensity and shape for the PMMA/TiO₂ composite become maximum and sharp respectively for 0.1wt% TiO₂ content and the 2925 cm⁻¹ peak's intensity become less intense with addition of TiO₂. These changes in these peaks are the indication of the PMMA's interactive role with TiO₂ [31].

There are noticeable changes in above peaks in intensity as shown in **Figure 6.1 (a)**. Noticeable peaks sharpening and shape changing is indicating the bonding like interaction between PMMA and TiO₂ particles. These changes are observed maximum for 0.1wt% of TiO₂, that provide a proof for the strong bond (increasing bond strength) interaction and there for the mechanical and thermal properties are prominent for 0.1wt% of TiO₂.

6.2.2. UV-Vis Analysis

The absorption spectra of most organic composites in the visible and near-UV region are broadband and contain one or several maxima depending upon the electron transition as suggested by Krasovitskiĭ and Bolotin [32]. The various optical properties obtained for different samples are listed in **Table 6.2**. Absorption coefficient (α) vs wavelength (λ), plot is shown in **Figure 6.2 (a)**. From **Figure 6.2 (a)** we can see a sharp increase of light absorption below 250 nm, which corresponds to $\pi \rightarrow \pi^*$ transitions of carbonyl groups in macromolecules [33]. And the presence of a weak absorption peak at near 276 nm, is considered to be a positive identification of carbonyl group which is corresponds to $n \rightarrow \pi^*$ transition of aldehydic carbonyl group of PMMA polymer. But the intensity of this peak decreases with increase in the doping percentage and at higher doping percentage it disappears. Light absorption increases as TiO₂ percentage increases, in comparison to pure PMMA. These spectra show the transitions of the electrons from a fundamental level to the excited levels. In absorption spectra, small peaks can be observed beside the fundamental maxima, showing the vibrational transitions in the structure of materials. Optical absorption studies on pure and doped films were carried out to determine the optical constants such as optical band gap (E_g) and the position of the fundamental band edge. According to Shahada et al. [34], it was observed that two distinct linear relations were found, corresponding to different inter band absorption processes. The lower energy range of $x = 2$ is

typical of an indirect allowed transition. The indirect optical energy gap can be obtained from the plot of $(\alpha h\nu)^{1/2}$ versus $h\nu$, while the direct energy gap, $x = 1/2$, can be obtained from the plot of $(\alpha h\nu)^2$ versus $h\nu$, is believed to be appropriate for the higher energy absorption. The position of the absorption edge was calculated by extrapolating the linear portions of α vs $h\nu$ plots (**Figure 6.2 (b)**) to zero absorption value. For pure film, the absorption edge lies at 4.50 eV and for doped films, the values are found to increase from 4.50 to 4.92 eV. Values of its absorption edge for 0.1 % of TiO_2 lies at 4.85eV above pure PMMA. The plots of $(\alpha h\nu)^2$ versus $h\nu$ for different dopant percentage in polymer are shown in **Figure 6.2 (c)**. The intercept on the energy axis on extrapolating the linear portion of the curves to zero absorption value may be interpreted as the value of the band gap. The values obtained for direct band gap, E_g for the different percentage of TiO_2 samples are found to be nonlinear. For pure PMMA, the direct band gap lies at 4.53 eV while for doped films, the values are found to vary with doping percentage as shown in **Table 6.2**. Its values are found to increase from 4.53 eV to 5.01 eV. The indirect band gap were obtained from the plot of $(\alpha h\nu)^{1/2}$ vs $h\nu$ (photon energy), as shown in **Figure 6.2 (d)**, should be linear. For pure PMMA, the indirect band gap lies at 4.44 eV while for doped films, the values are found to increase from 4.44 eV to 4.84 eV.

Table 6.2 Various of absorption edge and direct/indirect band gap with different blend percentage

TiO ₂ Percentage (%)	Absorption edge (ΔE) (eV)	Direct band gap ($E_{g(\text{Dir})}$)	Indirect band gap ($E_{g(\text{Indir})}$)
0%	4.50	4.53	4.44
0.03%	4.91	5.01	4.84
0.1%	4.85	4.97	4.78
0.5%	4.92	4.99	4.72

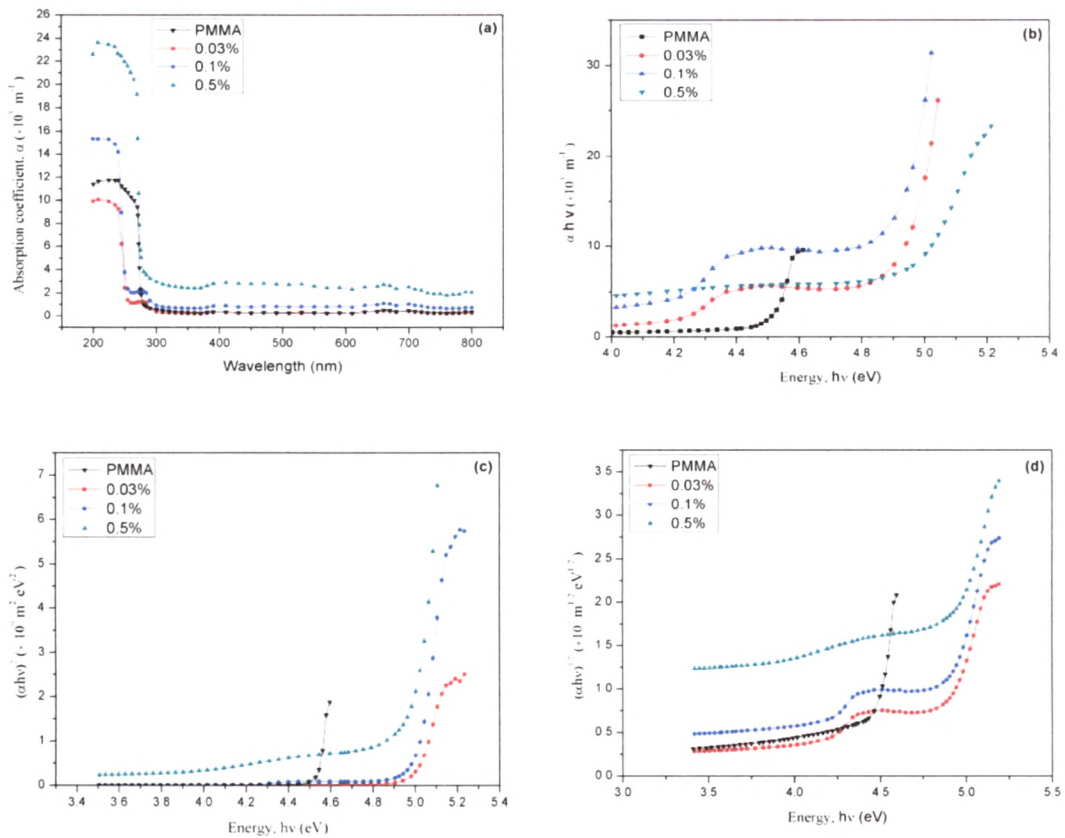


Figure 6.2 Plot of (a) Absorption coefficient (α) vs Wavelength (λ), (b) Absorption coefficient (α) vs Photon Energy ($h\nu$), (c) $(\alpha h\nu)^2$ vs $h\nu$, (d) $(\alpha h\nu)^{1/2}$ vs $h\nu$

6.2.3. Mechanical Analysis

The mechanical properties of the composite films such as elongation at break, Young's modulus, stress at break and ultimate tensile strength as a function of weight fraction of TiO_2 are displayed in **Figure 6.3 (a, b)**. The mechanical properties of the composite films such as ultimate tensile strength, elongation at break, etc. as a function of weight fraction of TiO_2 are displayed as graph (**Figure 6.3 (a, b)**). Due to introduction of TiO_2 particles into PMMA matrix, the values of mechanical properties such as ultimate tensile strength, Young's modulus and stress at break of composites exhibit increase up to the extent 0.1% of TiO_2 , beyond which it tends to decrease.

The difference in these values, in PMMA/TiO₂ composites are due to the difference in cross linking density provided by PMMA with different weight fraction values of TiO₂. In general polymers having either a high degree of crystallinity, cross linking or rigid chain exhibit a high strength and low extendibility, thereby giving a high Young's Modulus (YM) values, high stress at peak value and low elongation value [35]. This is also true in this case. Maximum value of the mechanical properties obtained for the 0.1% TiO₂ composites due to the strong bond interaction between PMMA matrix and TiO₂, while in other cases this interaction may be weak. Beyond 0.1%, mechanical properties value decreases because, increasing amount of TiO₂ particles makes it more difficult for dispersion and easier for particles agglomeration. Since agglomerated particles makes possible to generate defects in the composites, so stress concentration occur within PMMA matrix, resulting in a decreased tensile strength and other properties.

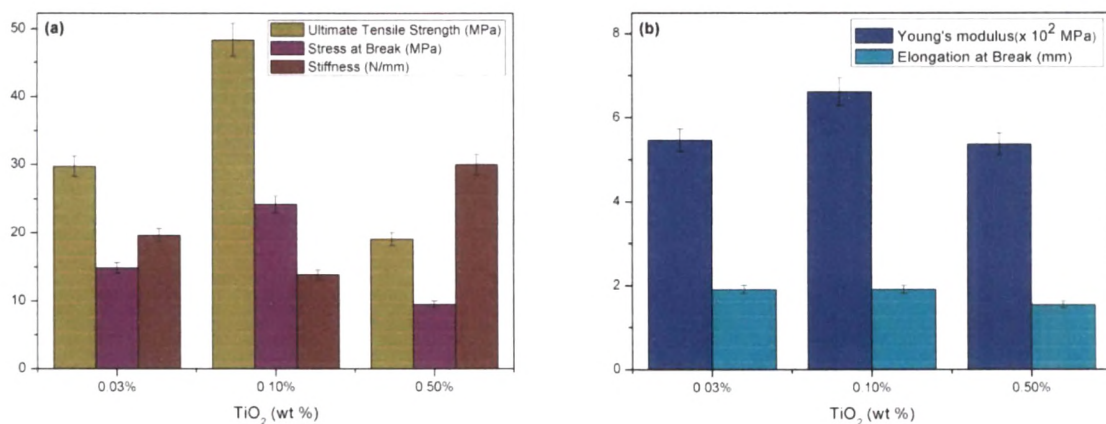


Figure 6.3 Variation in Ultimate tensile strength, stress at break, Stiffness, Young's Modulus, Elongation at break as a function of TiO₂ content

6.2.4. Differential Scanning Calorimeter Analysis

The glass transition behavior of the synthesized PMMA/TiO₂ samples was investigated by DSC. The obtained DSC thermograms are shown in **Figure 6.4 (a)**. The values of glass transition temperature were taken as the midpoint of the glass transition event. The obtained results are collected in **Table 6.3**. At the glass transition temperature, the bonds between TiO₂ and the polymer chains are broken, and the macromolecule starts to move. In **Figure 6.4**, shifting of T_g implies that PMMA and TiO₂ have miscibility in amorphous state. T_g of the pure PMMA sample is observed at 65.5 °C and it is maximum for 0.1% TiO₂ at 67.2°C. This implies that there is a strong bond interaction and good dispersibility between PMMA and TiO₂ in this composition.

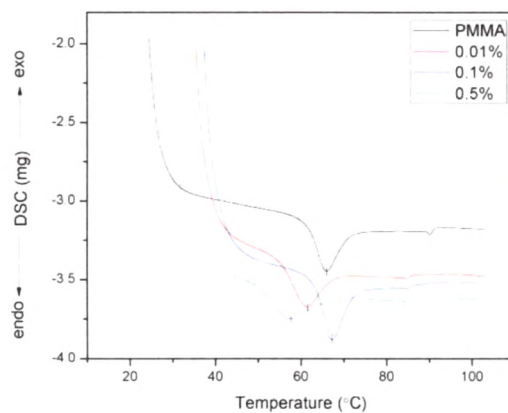


Figure 6.4 DSC curve for PMMA and its composites.

Table 6.3 Glass Transition temperature (T_g) °C of different PMMA/ TiO₂ Composites.

TiO ₂ % in PMMA	T _g (°C)
0 %	65.6
0.03 %	61.2
0.1 %	67.2
0.5 %	57.5

6.2.5. Thermal gravimetric Analysis

The thermal stability of the synthesized composite samples was studied by non-isothermal thermogravimetry. The Thermo gravimetric (TG) and derivative thermo gravimetric (DTG) curves obtained for the pure PMMA and PMMA/TiO₂ samples in nitrogen atmosphere are shown in **Figure 6.5 (a, b)**. The difference in the thermal decomposition was observed clearly from derivative TG (DrTG) curve as shown in **Figure 6.5 (b)**. The initial weight loss was observed for all samples due to moisture evaporation. The major weight losses occurred in the range of 260 – 430 °C for all the composite samples. It can be noticed from the TG curves in **Figure 6.5 (a)** that the composite samples start losing mass at lower temperature (at about 260 °C) than the pure PMMA sample. The onset of mass loss of composite samples is shown in **Table 6.4**. Also, the onset of mass loss is maximum for 0.1% of TiO₂ in composite samples. In comparison to composites samples 0.1 % of TiO₂ is also more stable than other composites, which clearly proved by peak temperature (Tp) value of degradation peak as shown **Table 6.4**. It is well studied by Kashiwagi et. al.[36] that PMMA thermally decomposes in steps, first degraded scissions at chain end initiation from unsaturated end groups and then most stable step degraded by random scission with in the mail polymer chain. [37]. The DTG curve of pure PMMA (**Figure 6.5 (b)**) has a peak at 378 °C, which corresponds to depolymerization initiated by random main chain scission and a peak at 308 °C which corresponds to depolymerization initiated by unsaturated end group.[38]. The DTG curves of 0.03% of TiO₂ composites also contain one small hump like peak at 280 °C while for 0.1% and 0.5 % composites shows one peak at 353 °C and 342 °C respectively, originating from the depolymerization initiated by random main chain scission. These results show that amount of PMMA chains with double bond at the end are larger in the pure PMMA than in the composites samples. So TiO₂ particles may

be react with unsaturated end groups of PMMA. As a result of it the number of unsaturated end groups is reduced.

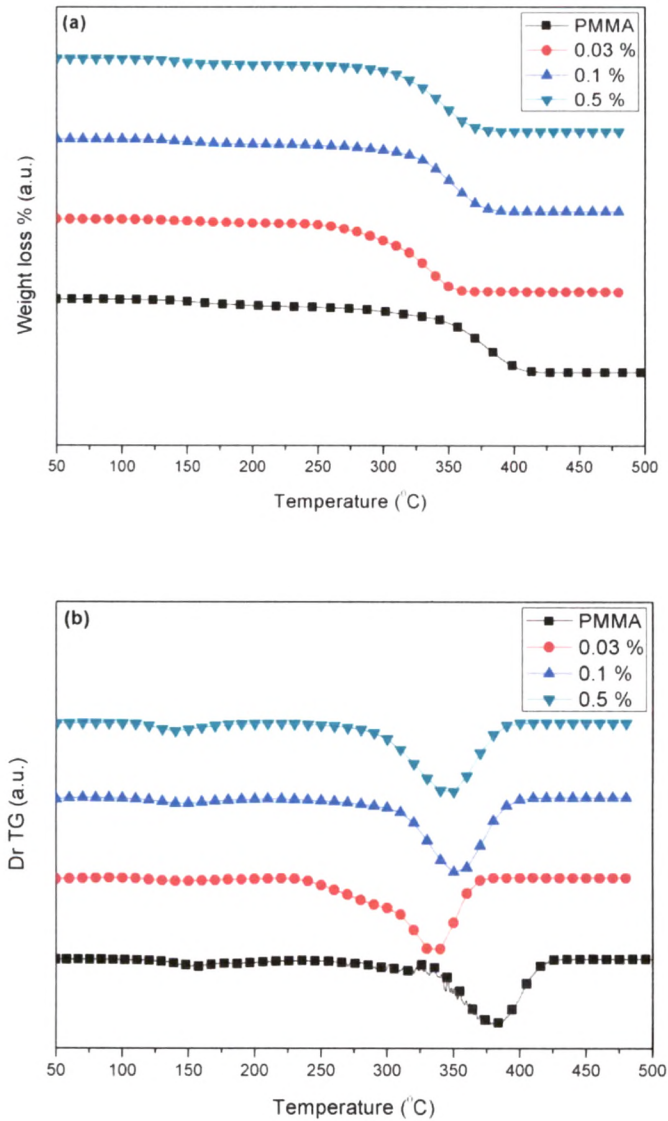


Figure 6.5 (a) TG of pure PMMA and their composites (b) Derivative TG of pure PMMA and their composites

Table 6.4 TG and DrTG data of Pure PMMA and their composites

TiO ₂ wt % in PMMA	Temperature(°C)		
	Starting	Ending	T _p
0/100	325	426	378
0.03%	260	369	336
0.1%	300	400	353
0.5%	289	389	342

6.2.6. Scanning Electron Microscopy

For organic/inorganic hybrid materials, dispersion of inorganic dopant in organic materials is very important to study the properties of composites materials. So, microscopic study on cross section of composite samples was conducted using SEM. **Figure 6.6** shows SEM micrographs of PMMA (**Figure 6.6 (a)**) and its composites with different TiO₂ weight contents (**Figure 6.6 (b-d)**). From SEM image for PMMA (**Figure 6.6 (a)**), smooth and homogeneous surface with some straps obtained. TiO₂ particles disperse differently in the polymer matrix with different percentage filler as shown in **Figure 6.6 (b-d)**. PMMA polymer and the TiO₂ fillers proved homogeneous and compatible without any phase separation occurring when a 0.1% of TiO₂ fillers was added in PMMA polymer matrix. While for 0.5% of TiO₂, the surface morphology of the composite polymer sample shows many clusters or chunks randomly distributed. That's why 0.1 % of TiO₂ have good mechanical and thermal properties compared to others.

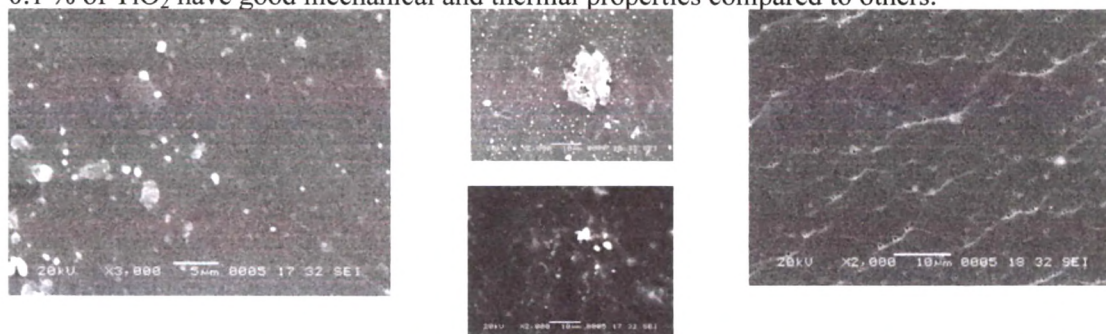


Figure 6.6 Scanning Electron Micrograph of (a) Pure PMMA (b) 0.03% (c) 0.1% (d) 0.5% of TiO₂

6.3. Conclusions

Mechanical, Thermal and Structural studies have been carried out to characterize PMMA/TiO₂ polymer composites. The FTIR analysis clearly shows that -COOCH₃ group of PMMA bonding with the TiO₂. When 0.1 wt% TiO₂ is added to PMMA polymer system, strong interaction is formed between PMMA and TiO₂. Which results in maximum values of mechanical properties such as young's modulus, Ultimate tensile Strength etc. and thermal properties of PMMA/TiO₂ composites. From DSC study, miscibility behavior of PMMA/TiO₂ composites is proved. Glass transition temperature is also maximum for 0.1 wt% of TiO₂. From UV-Vis spectra, the optical band gap (E_g) (Direct and Indirect) is found to be compositional dependence. The optical energy gap is less for 0.5% TiO₂ composition. From SEM micrograph, homogeneous and compatible without any phase separation occurring when a 0.1% of TiO₂ fillers was added in PMMA polymer matrix. From above conclusion for just 0.1% of TiO₂ cause changes in PMMA polymer matrix and enhancing thermal and mechanical properties.

6.4. References

1. Sun YP, Hao EC, Zhang X et al, *Langmuir* 13:5168–5174, 1997.
2. Pinnavaia TJ, Beall GW *Polymerclay nanocomposites*. John Wiley and Sons, New York, 2001.
3. Wei Li, Hong Li, Yong-Ming Zhang, *J Mater Sci* 44:2977–2984, 2009.
4. Mingjiao Yang, Yi Dan, *Colloid Polym Sci* 284: 243–250, 2005.
5. Meneghetti P and Qutubuddin S *Langmuir* 20 3424, 2004.
6. Mark J E *Polym. Eng. Sci.* 36 2905, 1996.
7. Qiang X, Chunfang Z, Zun Y J and Yuan C S *J. Appl. Polym. Sci.* 91 2739, 2004.
8. Kicelbick G. *Prog Polym Sci* ;28(1):83–114, 2003.
9. Rohan L. Holmes, Jonathan A. Campbell, Robert P. Burford, Inna Karatchevtseva, *Polymer Degradation and Stability*, 94. 1882–1889, 2009.
10. Demjén, Z., Pukánszky, B. & Nagy, J. *Compos. Part A*, 29, 323–329, 1998.
11. Acosta JL, Morales E *Solid State Ion* 85:85. 1996. [2] Kim JY, Kim SH *Solid State Ion* 124(1–2):91, 1999.
12. C.A. Linkous, *Environ. Sci. Technol.* 34, 44754, 2000.
13. A. Fujishima, T.N. Rao, D.A. Tryk, *J. Photochem. Photobiol. C1*, 1, 2000.
14. P. Loebel, M. Huppertz, D. Mergel, *Thin Solid Films* 251, 72, 1994.
15. I. Hayakawa, Y. Iwamoto, K. Kikuta, *Sens. Actuators B* 62, 55, 2000.
16. A. Hagfeld, B. Didriksson, *Sol. Energy Mater. Sci. Cells* 31, 481, 1994.
17. S.A. Carter, J.C. Scott, P.J. Brock, *Appl. Phys. Lett.* 31, 1145, 1997.
18. J. Zhang, X. Ju, B. Wang, Q. Li, T. Liu, T. Hu, *Synth. Metals* 118, 181, 2001.
19. Abd E I, Kader F H, Osman W H, Ragab H S, Sheap A M, Rizk M S & Basha M A F, *J polym Matter*, 21, 49, 2004.

20. Ma H L, Zhang X H & Lucas J, *J Non-cryst solids*, 101, 128, 1993.
21. A. Qureshi, Dolly Singh, N.L. Singh, S. Ataoglu, Arif N. Gulluoglu, Ambuj Tripathi, D.K. Avasthi *Nuclear Instruments and Methods in Physics Research B* 267 3456–34, 2009.
22. J.M. Ziman, in *Principles of the Theory of Solids* (Cambridge University Press, Cambridge, 1979).
23. H.M. Zidan, M. Abu-Elnader, *Physica B*. 355, 308, 2005.
24. V. Švorčík, I. Miček, V. Rybka, V. Hnatowicz, *J. Mater. Res.* 12, 1661, 1997.
25. R. Mishra, S.P. Tripathy, D. Sinha, K.K. Dwivedi, S. Ghosh, D.T. Khathing, M. Muller, D. Fink, W.H. Chung, *Nucl. Instrum. Meth. B*. 168, 59; 2000.
26. Vijay V. Soman and Deeplai S. Kelkar, *Macromol. Symp.*, 277, 152-161, 2009.
27. S. York, R. Frech, A. Snow, D. Glatzhofer, *Electrochim Acta*, 46, 1533, 2001.
28. A. P. Rhode, R. Frech, *Solid State Ionics*, 121; 91, 1999.
29. Jiao Wang, Xiuyuan Ni, *Journal of Applied Polymer Science*, Vol. 108, 3552–3558, 2008.
30. Annalisa Convertino, A.; Gabriella Leo, A., Marinella Striccoli, B.; Gaetano Di Marco, C.; Lucia Currib, M. *Polymer*, 49, 5526-5532, 2008.
31. Ahmad S, Saxena TK, Ahmad S et al , *J Power Sources* 159:205–209, 2006.
32. B. M. Krasovitskiĭ and B. M. Bolotin, *Organic Luminescent Materials*, 2nd ed. (Khimiya, Moscow, 1984; VCH, Weinheim, 1988).
33. M. Hammama, M.K. El-Mansy, S.M. El-Bashir, M.G. El-Shaarawy, *Desalination* 209, 244, 2007.
34. L. Shahada, M. E. Kassem, H. I. Abdelkader, and H. M. Hassan, *J. Appl. Polym. Sci.* 65, 1653, 1997.

-
35. Kim Chi S and Oh Seung M, *Electrochim Acta.*, 46,1323-31, 2001.
 36. T. Kashiwagi, A. Inaba, J.E. Brown, K. Hatada, T. Kitayama, and E. Masuda, *Macromolecules*, 19, 2160-2168, 1986.
 37. L. Katsikas, J.S. Velickovic, H. Weller, and I.G. Popovic, *J. Therm. Anal.*, 49, 317, 1997.
 38. E. Dz̃ unuzovic' , M. Marinovic' -Cincovic', J. Vukovic', K. Jeremic', J.M. Nedeljkovic' *POLYMER COMPOSITES*—737-742, 2009.